Environmental Surveillance and Transmission Risk Assessments for SARS-CoV-2 in a Fitness Center

Hongwan Li[1], Sripriya Nannu Shankar[1], Chiran T. Witanachchi[1], John A. Lednicky[2,3], Julia C. Loeb[2,3], Md. Mahbubul Alam[2,3], Z. Hugh Fan[4,5], Karim Mohamed[5], Arantzazu Eiguren-Fernandez[6], and Chang-Yu Wu[1]*

[1] Department of Environmental Engineering Sciences, University of Florida, USA
[2] Department of Environmental and Global Health, University of Florida, USA
[3] Emerging Pathogens Institute, University of Florida, USA
[4] Department of Mechanical & Aerospace Engineering, University of Florida, USA
[5] J. Crayton Pruitt Family Department of Biomedical Engineering, University of Florida, USA
[6] Aerosol Dynamics Inc., Berkeley, California, USA

*Corresponding author at: Tel: 1-352-392-0845; E-mail: cywu@essie.ufl.edu

Supplementary Material

Supplementary figure

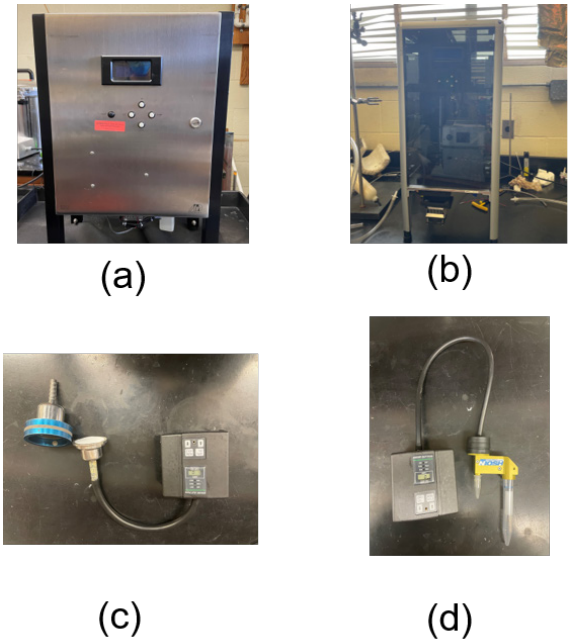

Figure S1. Four samplers deployed to collect air samples in the fitness center: (a) BioSpot-VIVAS; (b) VIVAS; (c) an in-line holder for PTFE filter; (d) NIOSH BC-251 bioaerosol sampler.

Section S1. Limit of detection of air samples

The LOD of the rRT-PCR detection system is ~1.5 SARS-CoV-2 genome equivalents per 25 µL rRT-PCR assay. Accordingly, the number of virus genome equivalents in 140 µL (volume of collection media from which RNA was purified) of the detection limit, N_{140}, is:

$$N_{140} = 1.5\ (virus\ genome\ equivalents\ in\ PCR\ assay) \times \frac{80\ \mu L\ (volume\ of\ total\ RNA\ purified\ from\ 140\ \mu L\ collection\ medium)}{5\ \mu L\ (tested\ volume\ in\ PCR\ assay)} = 24\ viral\ genome\ equivalents /140\ \mu L\ (collection\ medium) \quad (1)$$

As an example, for BioSpot-VIVAS and VIVAS air samples, the total amount of virus genome equivalents in the collection medium is:

$$N = 24 \times \frac{1489\ \mu L(total\ volume\ collected)}{140\ \mu L(total\ volume\ tested)} = 255\ viral\ genome\ equivalents \quad (2)$$

The concentration of virus in the air samples is:

$$C = \frac{255\ viral\ genome\ equivalents}{3h \times 8\frac{L\ of\ air}{min} \times 60\frac{min}{h}} = 0.18\ \frac{viral\ genome\ equivalents}{L\ of\ air} \quad (3)$$

Results of LOD for other samples are shown in Table S1.

Table S1. LOD for air samples

	BioSpot -VIVAS /VIVAS	Millipore/ NIOSH BC-251 filters	NIOSH 15 mL centrifuge tube for >4.4 μm particles	NIOSH 1.5 mL centrifuge tube for 1.1-4.4 μm particles
Total volume of collection medium, μL	1489	1500	1500	500
Total amount of SARS-CoV-2 genome equivalents	255	257	257	86
Air sampling flow rate, L min^{-1}	8	3	3	3
Sampling time, h	3	1	1	1
Air volume, L	1440	180	180	180
LOD, SARS-CoV-2 genome equivalents/L of air	0.18	1.43	1.43	0.48

Section S2. Assumptions in the Wells-Riley equation

There are several assumptions in the Wells-Riley equation: (a) there is no prior infectious respiratory aerosol at the initial time point (t = 0); (b) the rate of quanta emission rate is steady; (c) the infectious quanta are reduced by first-order decay progress due to the sum of ventilation, recirculation, filtration, air disinfection, deposition, and viral aerosol inactivation; (d) characteristics of the exposed population are not included in the risk model, such as the person's age, vaccination history, and underlying health problems; (e) risk of infection is based on airborne transmission.

Section S3. Determination of the quanta emission rate

There are a few studies that have reported the estimated values of quanta emission rate. Miller et al. (2020) assessed the emission rate of 970 quanta h^{-1} for singing activity, based on the infection rate in a choir rehearsal outbreak. Based on viral load in the sputum, Buonanno et al. (2020) derived a function to estimate the emission rate from <1 quanta h^{-1} to >100 quanta h^{-1}, at different activity levels. Harrichandra et al. (2020) applied that model with a modified breathing rate and used the emission rate of 142 quanta h^{-1} to estimate the infection risk in nail salons. Dai and Zhao (2020) fitted a curve between emission rate and airborne disease reproductive number, including Tuberculosis, MERS, SARS, Influenza, and Measles, to obtain 14-48 quanta h^{-1} at light activity levels. Kriegel et al. (2020) implemented the previous model with measurements of particle emission rate and breathing rate at different activity levels, and they reported 139 quanta h^{-1} for light exercise. Assuming it depends on aerosol emission rates and breathing rates at different activity levels (Kriegel et al., 2020a), the average quanta emission rate can be written as

$$E = E_0 \cdot \frac{\sum_{i=1}^{4}(N_{i,j} \cdot V_i)}{\sum_{i=1}^{4}(N_{i,o} \cdot V_i)} \cdot \frac{Q_b}{Q_{b,o}} \quad (4)$$

where E_0 (quanta h^{-1}) is the reference quanta emission rate and can be found in the aforementioned studies; N_j and N_0 (particles cm^{-3}) are the emitted particle number concentrations at unmodulated vocalization (i.e., assumed expiratory activity as baseline conditions in the fitness center) and reference expiratory activity (e.g., voice counting, beathing, and singing), respectively (Morawska et al., 2009); V_i (cm^3) is the volume of a single particle and *i* refers to four particle sizes (Morawska et al., 2009); Q_b and $Q_{b,0}$ (m^3 h^{-1}) are the breathing rates at heavy exercise, 3.3 m^3 h^{-1}, and reference activity levels, respectively (Morawska et al., 2009). Applying the estimated values from previous studies to Equation 4, the average emission rate of

896 quanta h^{-1} is obtained, and details are shown in Table S2. If more than one person exercising in the site is infectious, the inferred quanta emission rates would be the sum of all individual emission rates.

Table S2. Calculated emission rates at heavy exercise

Activity	Expiratory activity	Breathing rate (Q_b), m^3 h^{-1}	Emission rate (E_0), quanta h^{-1}	$(\frac{\sum_{i=1}^{4}(N_{i,j}\cdot V_i)}{\sum_{i=1}^{4}(N_{i,o}\cdot V_i)})$(Morawska et al., 2009)	Reference	Calculated emission rate at heavy exercise (E), quanta h^{-1}
Light	Unmodulated vocalization	0.96	142	1	Harrichandra et al. (2020)	488
Heavy	Unmodulated vocalization	3.3	733	1	Buonanno et al. (2020)	733
Light	Unmodulated vocalization	0.54	139	1	Kriegel et al. (2020a)	849
Light	Voice counting	0.3	14	6.41 (Morawska et al., 2009)[a]	Dai and Zhao (2020)	987
Singing	Singing	1	970	0.45 (Kriegel et al., 2020b; Morawska et al., 2009)[b]	Miller et al. (2020)	1424

[a].Calculated from particle generation during unmodulated vocalization and voice counting (Morawska et al., 2009).

[b].Calculated from the median values of particle generations for singing and voice counting as 1923/133=14.4 (Kriegel et al., 2020b); and based on the ratio of particle generations for voice counting and unmodulated vocalization (i.e., 6.41), calculated the ratio of particle generations for singing and unmodulated vocalization as 6.41/14.4=0.45 (Morawska et al., 2009).

Section S4. Sensitivity analysis of infection risk

The infection risk P_i is based on the estimated quanta emission rate when patrons vocalize in unmodulated voice. Among the four expiratory activities (i.e., breathing, whispered counting, voiced counting, and unmodulated vocalization) that generate different size distribution of particles (Morawska et al., 2009), unmodulated vocalization was conservatively used for fitness center patron expiratory activities. Buonanno et al. (2020) assumed the expiratory activity for patrons in a gym at the breathing level, resulting in the median quanta emission rate of 2.5

quanta h^{-1} $person^{-1}$. If this quanta value were used, the P_i is calculated as 0.005% at the visited fitness center, which is much lower than the P_i when the infected patron conducts unmodulated vocalization activities (E = 896 quanta h^{-1} $person^{-1}$).

As a baseline assessment in the fitness center, the β_{dep}= 0.3 h^{-1} measured by Thatcher et al. (2002) was used, although a higher value of 1.5 h^{-1} was reported by Diapouli et al. (2013). The β_{ina} = 0.63 h^{-1} measured by van Doremalen et al. (2020) was used for the estimations, corresponding to the 1.1 h half-life of aerosolized virus, whereas a minimal decay for virus-laden aerosols after 16 hours reported by Fears et al. (2020) resulting in β_{ina} = 0 h^{-1} would contribute to P_i =1.87%, which is slightly higher than that calculated by β_{ina} = 0.63 h^{-1} (van Doremalen et al., 2020). As this assessment aims to investigate the effectiveness of ventilation in reducing the airborne SARS-CoV-2 transmission, the quanta emission rate at the unmodulated voice level and decay rate of 0.63 h^{-1} (van Doremalen et al., 2020) were adopted for the baseline examinations.

Section S5. Virus inactivation efficiency of the UVGI unit in the fans

Figure S2 displays the schematic diagram of the UVGI unit installed in the upper room with its dimensions. The UVC lamp is 9 watts, and air is drawn by a fan through the UVGI unit at a flow rate, Q_r, of 930 m^3 h^{-1}. Based on Figure S2, the air velocity υ_r (m s^{-1}) at the cross-section is:

$$v_r = \frac{Q_r}{A_{cross-section}} = \frac{4 \cdot Q_r}{\pi \cdot D_r^2} = \frac{4 \times 930\ m^3/h}{\pi \cdot (0.325m)^2} = 11216\frac{m}{h} = 3.12\frac{m}{s} \qquad (5)$$

where $A_{cross\text{-}section}$ (m^2) is the cross-sectional area of the air flow; D_r = 0.325 m is the diameter of the cross-sectional area. The residence time τ_r (s) of room air passing through the UVGI is:

$$\tau_r = \frac{L_r}{v_r} = \frac{0.311\ m}{3.12\ m/s} \approx 0.1\ s \qquad (6)$$

where L_r = 0.311 m is the length of the UVC lamp.

The median intensity can be approximated at the circular side at $R_{r,50}$ (Figure S2), which is the radius corresponding to half of the cross-sectional area defined as:

$$\frac{\pi R_r^2}{2} = \pi(\frac{R_r}{\sqrt{2}})^2 = \pi R_{r,50}^2 \qquad (7)$$

Accordingly, $R_{r,50}$ is determined as:

$$R_{r,50} = \frac{R_r}{\sqrt{2}} = \frac{32.5\ cm/2}{\sqrt{2}} = 11.49\ cm \qquad (8)$$

The median intensity $I_{r,50}$ of the UVC lamp is calculated by:

$$I_{r,50} = \frac{P_r}{A_{r,50}} = \frac{P_r}{2\pi R_{r,50} L_r} = 4010\,\frac{\mu W}{cm^2} \qquad (9)$$

where P_r = 9 watts is the power of UVC lamp; $A_{r,50}$ is the tubular area at radius of $R_{r,50}$.

The median virus inactivation efficiency $\eta_{r,50}$ (unitless) can be described as (Tseng et al., 2005):

$$\eta_{r,50} = 1 - e^{-kI_{r,50}t} \qquad (10)$$

where k ($cm^2\ mW^{-1}\ s^{-1}$) is the UV inactivation rate constant or susceptibility factor, and the values (0.0081, 0.0041, and 0.0059) were obtained from studies of UVC inactivation for airborne single strand bacteriophage MS2 and human coronaviruses (Buonanno et al., 2020; Tseng et al., 2005). The values of $\eta_{r,50}$ corresponding to the three k's are 0.961, 0.807, and 0.906. Therefore, the calculated mean virus inactivation efficiency $\overline{\eta_{r,50}}$ = 89.1%.

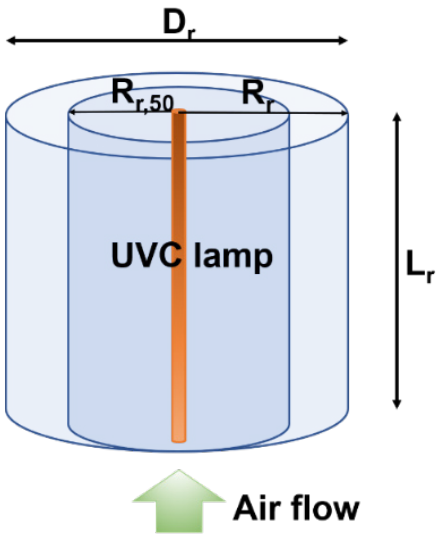

Figure S2. Schematic figure of UVC dose in upper room UVGI

Section S6. Virus inactivation efficiency of the UVGI unit in the AHU

There are 12 AHUs in the HVAC system at the visited fitness center, and details of AHU dimensions are shown in Table S2. The calculation of the virus inactivation efficiency in Main area 1 is shown here as an example, at 10 ACH with 36% air recirculation (conditions of the visited fitness center). Calculations of other areas can be obtained using the same method with the corresponding air flow rate listed in Table S3. For the Main area 1, the air velocity υ_A (m s^{-1}) at the AHU inlet surface ($H_A \times W_A$) (Figure S2), which is the same for all 12 areas, is:

$$v_A = \frac{Q_A}{A_{HW}} = \frac{12782\,\frac{m^3}{h}}{1.63\,m^2} = 7842\,\frac{m}{h} = 2.18\,\frac{m}{s} \qquad (11)$$

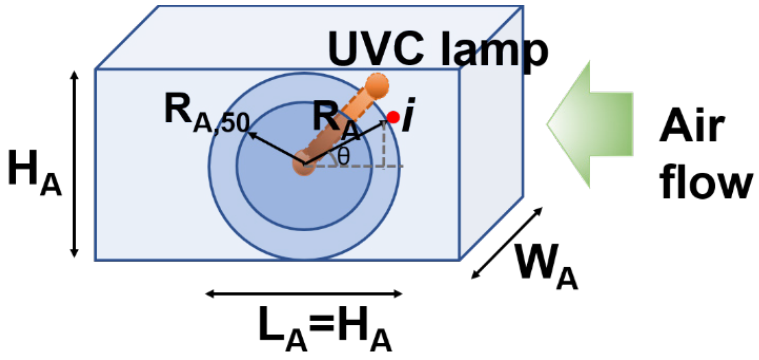

Figure S3. Schematic figure of UVC dose in the UVGI inside AHU

Assuming the UV dose is circularly distributed around the lamp, the median intensity occurs at the circle with $R_{A,50}$, following the same approach in Section S5 i.e.,

$$R_{A,50} = \frac{R_A}{\sqrt{2}} = \frac{76\ cm/2}{\sqrt{2}} = 26.87\ cm \qquad (12)$$

The median intensity $I_{A,50}$ is calculated by:

$$I_{A,50} = \frac{P_A}{A_{A,50}} = \frac{P_A}{2\pi R_{A,50} W_A} = \frac{144\ W}{2\pi \cdot 26.87cm \cdot 213cm} = 4006 \frac{\mu W}{cm^2} \qquad (13)$$

If one air stream enters AHU at point *i* (Figure S2), with degree of θ to the center horizontal surface, the residence time $\tau_{A,i}$ is:

$$\tau_{A,i} = \frac{2 \times R_A cos\theta}{v_A} \qquad (14)$$

The weighted residence time τ_A for total air flow is:

$$\tau_A = \frac{\int_0^{\frac{\pi}{2}} \frac{2R_A cos\theta d\theta}{v_A}}{\int_0^{\frac{\pi}{2}} \theta} = \frac{2R_A}{v_A} \times \frac{1}{\frac{\pi}{2}} = \frac{4R_A}{\pi v_A} = 0.22\ s \qquad (15)$$

The median virus inactivation efficiency $\eta_{A,50}$ (unitless) can be described as (Tseng et al., 2005):

$$\eta_{A,50} = 1 - e^{-kI_{A,50}\tau_A} \qquad (16)$$

The values of $\eta_{A,50}$ corresponding to the three k, obtained in Section S5 are 0.999, 0.974, and 0.995, respectively. Therefore, the calculated average virus inactivation efficiency in Main area unit 1 is $\overline{\eta_{A,50}}$ = 98.9%.

On the basis of the averaged virus inactivation efficiency in each AHU, the summed efficiency of UVGI in AHU can be obtained by:

$$\eta_A = \frac{\sum_{i=1}^{i=12}(\overline{\eta_{Ai,50}} \times Q_{re,i})}{Q_{re}} = 98.2\ \% \qquad (17)$$

Section S7. Infection risk assessment when wearing a face mask

If a patron wears a cloth mask in the fitness center, the Wells-Riley equation can be defined as (Bazant and Bush, 2021):

$$P_i = 1 - e^{-Q_b \int_0^T C(t) p_m dt} \qquad (18)$$

where p_m is the face mask penetration factor. Konda et al. (2020) measured the aerosol filtration efficiency FE= 54-95% for a wide range of cloth masks using common fabrics (e.g., cotton quilt, hybrid-cotton, and double-layer fabrics). As p_m=1-FE, the values of p_m using cloth mask would be 5-46%. Using a conservative penetration factor of 50% would provide a baseline assessment for using masks in reducing the airborne transmission of SARS-CoV-2.

Table S3. Details of 12 AHU dimensions

	Basketball unit	Group X unit	Main area		Dumbbell unit	Pool unit	Office Unit	PT unit	Extra unit 1		Extra unit 2	
			1	2					coil 1	coil 2	coil 1	coil 2
Coil H_A, m	0.61	0.99	0.76		0.76	1.17	0.56	1.09	0.76		0.76	
Coil W_A, m	1.78	0.91	2.13		2.24	1.93	1.37	1.6	2.62		2.62	
$H_A \times W_A$, m^2	1.08	0.91	1.63		1.7	2.26	0.77	1.75	1.99		1.99	
sum of $H_A \times W_A$, m^2	19.69											
Ratio of $H_A \times W_A$/ (sum of $H_A \times W_A$)	0.06	0.05	0.08		0.09	0.11	0.04	0.09	0.1		0.1	
Total power of UVC lamps, W	72	90	144		144	288	57	144	144		144	

*Q_{re}: total flow rate of recirculated air

Table S4. Calculations of the virus inactivation efficiency for UVGI inside AHU at different ventilation rates

	Basketball unit	Group X unit	Main area		Dumbbell unit	Pool unit	Office Unit	PT unit	Extra unit 1		Extra unit 2	
			1	2					coil 1	coil 2	coil 1	coil 2
*ACH=10, 36% air recirculation (visited fitness center)**												
Total Q_{re}, m^3/h	154800											
Q in each AHU, m^3/h	8522	7122	12783		13392	17734	6026	13742	15674		15674	
Velocity, m/s**	2.18											
Residence time t_A, s	0.18	0.29	0.22		0.22	0.34	0.16	0.32	0.22		0.22	
Efficiency												
k=0.0081	0.987	1.000	0.999		0.999	1.000	0.988	1.000	0.997		0.997	
k=0.0041	0.887	0.995	0.974		0.969	1.000	0.893	0.992	0.948		0.948	
k=0.0059	0.957	1.000	0.995		0.993	1.000	0.960	0.999	0.986		0.986	
Average efficiency in each AHU	0.943	0.998	0.989		0.987	1.000	0.947	0.997	0.977		0.977	
Summed efficiency	98.2%											
ACH=10, 100% air recirculation												

	Basketball unit	Group X unit	Main area		Dumbbell unit	Pool unit	Office Unit	PT unit	Extra unit 1		Extra unit 2	
			1	2					coil 1	coil 2	coil 1	coil 2
Total Q_{re}, m^3/h	430000											
Q in each AHU, m^3/h	23672	19783	35508		37199	49260	16740	38171	43540		43540	
Velocity, m/s	6.07											
Residence time t_A, s	0.06	0.10	0.08		0.08	0.12	0.06	0.11	0.08		0.08	
Efficiency												
k=0.0081	0.788	0.977	0.925		0.915	0.997	0.796	0.968	0.879		0.879	
k=0.0041	0.544	0.852	0.730		0.713	0.945	0.553	0.825	0.656		0.656	
k=0.0059	0.677	0.936	0.848		0.834	0.984	0.686	0.919	0.785		0.785	
Average efficiency in each AHU	0.670	0.921	0.834		0.821	0.975	0.679	0.904	0.773		0.773	
Summed efficiency	82.0%											
ACH=5, 100% air recirculation												
Total Q_{re}, m^3/h	215000											
Q in each AHU, m^3/h	11836	9892	17754		18599	24630	8370	19086	21770		21770	
Velocity, m/s	3.03											
Residence time t_A, s	0.13	0.21	0.16		0.16	0.25	0.12	0.23	0.16		0.16	
Efficiency												
k=0.0081	0.955	0.999	0.994		0.993	1.000	0.959	0.999	0.985		0.985	
k=0.0041	0.792	0.978	0.927		0.918	0.997	0.800	0.969	0.882		0.882	
k=0.0059	0.896	0.996	0.977		0.973	1.000	0.902	0.993	0.954		0.954	
Average efficiency in each AHU	0.881	0.991	0.966		0.961	0.999	0.887	0.987	0.940		0.940	
Summed efficiency	95.4%											
ACH=1, 100% air recirculation												
Total Q_{re}*, m^3/h	43000											
Q in each AHU, m^3/h	2367	1978	3551		3720	4926	1674	3817	4354		4354	
Velocity, m/s	0.61											
Residence time t_A, s	0.64	1.04	0.80		0.80	1.23	0.59	1.15	0.80		0.80	

	Basketball unit	Group X unit	Main area		Dumbbell unit	Pool unit	Office Unit	PT unit	Extra unit 1		Extra unit 2	
			1	2					coil 1	coil 2	coil 1	coil 2
Efficiency												
k=0.0081	1.000	1.000	1.000		1.000	1.000	1.000	1.000	1.000		1.000	
k=0.0041	1.000	1.000	1.000		1.000	1.000	1.000	1.000	1.000		1.000	
k=0.0059	1.000	1.000	1.000		1.000	1.000	1.000	1.000	1.000		1.000	
Average efficiency in each AHU	1.000	1.000	1.000		1.000	1.000	1.000	1.000	1.000		1.000	
Summed efficiency	100%											

*Measured by the fitness center's contractor.

**Calculated by the measured flow rate divided by the cross-sectional area.

Table S5. Detailed characteristics of the visited fitness center

Location	North Central Florida
Site characterization	Residential area in an urban/suburban mix; Situated on ground level in an independent building; Two floors
Dimensions	
Area (m^2)	4658 (1st floor) & 2450 (2nd floor)
Height (m)	~ 3-9.4 (1st floor) & ~ 3-7 (2nd floor)
Total volume (m^3)	~ 43,000
Amenities	
Cardio equipment	Treadmills, AMTs, rowers, ellipticals, ARC trainers, stair climbers, etc.
Strength training	Free weights, deadlift platforms, squat racks, cables, and selectorized machines.
Studios	Indoor cycling (1), group classes (2), personal training (2)
Indoor basketball court	Regulation-size indoor basketball court
Indoor swimming pool	75-foot lap pool, warm thermal pool, and sauna
Others	Locker rooms (2), reception counter (1), and smoothies bar (1)
Occupancy (per day)	~2400 (pre-COVID-19)
	~1600 (during sampling periods)

References:

Bazant, M.Z., Bush, J.W.M. (2021). Beyond Six Feet: A Guideline to Limit Indoor Airborne Transmission of COVID-19. https://doi.org/10.1101/2020.08.26.20182824

Buonanno, G., Stabile, L., Morawska, L. (2020). Estimation of airborne viral emission: Quanta emission rate of SARS-CoV-2 for infection risk assessment. Environ. Int. https://doi.org/10.1016/j.envint.2020.105794

Buonanno, M., Welch, D., Shuryak, I., Brenner, D.J. (2020). Far-UVC light (222 nm) efficiently and safely inactivates airborne human coronaviruses. Sci. Rep. 10, 1–8. https://doi.org/10.1038/s41598-020-67211-2

Dai, H., Zhao, B. (2020). Association of the infection probability of COVID-19 with ventilation rates in confined spaces. Build. Simul. 13, 1321–1327. https://doi.org/10.1007/s12273-020-0703-5

Diapouli, E., Chaloulakou, A., Koutrakis, P. (2013). Estimating the concentration of indoor particles of outdoor origin: A review. J. Air Waste Manage. Assoc. 63, 1113–1129. https://doi.org/10.1080/10962247.2013.791649

Fears, A.C., Klimstra, W.B., Duprex, P., Hartman, A., Weaver, S.C., Plante, K.S., Mirchandani, D., Plante, J.A., Aguilar, P. V., Fernández, D., Nalca, A., Totura, A., Dyer, D., Kearney, B., Lackemeyer, M., Bohannon, J.K., Johnson, R., Garry, R.F., Reed, D.S., Roy, C.J. (2020). Persistence of Severe Acute Respiratory Syndrome Coronavirus 2 in Aerosol Suspensions. Emerg. Infect. Dis. 26, 2168–2171. https://doi.org/10.3201/eid2609.201806

Harrichandra, A., Ierardi, A.M., Pavilonis, B. (2020). An estimation of airborne SARS-CoV-2 infection

transmission risk in New York City nail salons. Toxicol. Ind. Health 36, 634–643. https://doi.org/10.1177/0748233720964650

Kriegel, M., Buchholz, U., Gastmeier, P., Bischoff, P., Abdelgawad, I., Hartmann, A., Kriegel, I.M. (2020a). Predicted infection risk for aerosol transmission of SARS-COV-2. medPxiv. https://doi.org/10.1101/2020.10.08.20209106

Kriegel, M., Lange, J., Hansj¨, H., Rotheudt, H., Fleischer, M. (2020b). Aerosol emission is increased in professional singing.

Miller, S.L., Nazaroff, W.W., Jimenez, J.L., Boerstra, A., Buonanno, G., Dancer, S.J., Kurnitski, J., Marr, L.C., Morawska, L., Noakes, C. (2020). Transmission of SARS-CoV-2 by inhalation of respiratory aerosol in the Skagit Valley Chorale superspreading event. Indoor Air 31, 314–323. https://doi.org/10.1111/ina.12751

Morawska, L., Johnson, G.R., Ristovski, Z.D., Hargreaves, M., Mengersen, K., Corbett, S., Chao, C.Y.H., Li, Y., Katoshevski, D. (2009). Size distribution and sites of origin of droplets expelled from the human respiratory tract during expiratory activities. J. Aerosol Sci. 40, 256–269. https://doi.org/10.1016/j.jaerosci.2008.11.002

Thatcher, T.L., Lai, A.C.K., Moreno-Jackson, R., Sextro, R.G., Nazaroff, W.W. (2002). Effects of room furnishings and air speed on particle deposition rates indoors. Atmos. Environ. 36, 1811–1819. https://doi.org/10.1016/S1352-2310(02)00157-7

Tseng, C.-C., Li, S., Li, C.-S. (2005). Inactivation of virus-containing aerosols by ultraviolet germicidal irradiation. Aerosol Sci. Technol. 39, 1136–1142. https://doi.org/10.1080/02786820500428575

van Doremalen, N., Bushmaker, T., Morris, D.H., Holbrook, M.G., Gamble, A., Williamson, B.N., Tamin, A., Harcourt, J.L., Thornburg, N.J., Gerber, S.I., Lloyd-Smith, J.O., De Wit, E., Munster, V.J. (2020). Aerosol and surface stability of SARS-CoV-2 as compared with SARS-CoV-1. New England Journal of Medicine. https://doi.org/10.1056/NEJMc2004973